2-1986

Optimum Shape Synthesis of Maximum Gain Omnidirectional Antennas

Frances J. Harackiewicz
University of Massachusetts - Amherst, fran@engr.siu.edu

David M. Pozar
University of Massachusetts - Amherst

Optimum Shape Synthesis of Maximum Gain Omnidirectional Antennas

FRANCES J. HARACKIEWICZ, STUDENT MEMBER, IEEE, AND DAVID M. POZAR, MEMBER, IEEE

Abstract—**Using characteristic mode shape synthesis, some antenna surfaces and their current distributions are found which produce maximum realizable gain for rotationally symmetric omnidirectional antennas. The same shape synthesis method fails to produce antennas which have maximum endfire gain.**

I. Introduction

The maximum realizable gain of an arbitrary antenna enclosed by a spherical surface has been discussed by Harrington [1], [2], [3] for the pencil beam (endfire) case and by Chu [4] for the omnidirectional (rotationally symmetric broadside) case. The maximum gain depends on N, the order of the highest spherical mode radiated by the antenna, and so is unbounded in general. To maintain a realizable gain (non-superdirective), the highest mode number should be constrained to be less than or equal to the electrical size ka of the enclosing spherical surface.

Now, by the equivalence theorem, an infinitude of surfaces (with equivalent currents) that circumscribe the spherical surface of size ka, produce the same pattern and maximum gain as the enclosed arbitrary antenna. Some of these surfaces are more desirable than others, however, since some of them radiate with a Poynting vector that is always directed normal to the antenna surface. That is, no power is directed back into the antenna, or along the antenna surface. These surfaces thus minimize loss into the antenna surface (and possibly minimize Q), and are called optimum shapes. The characteristic mode shape synthesis method of [5] and [6] is used to find these optimum shapes.

Two cases are considered. For the omnidirectional (broadside) case, transverse electric (TE) and transverse magnetic (TM) fields can be treated separately and identified with characteristic mode fields. Optimum shapes can then be determined, with corresponding fields and currents that produce maximum normal gain. For the pencil beam (endfire) case, however, the maximum gain fields cannot be identified with characteristic mode fields. Separating the maximum gain fields into characteristic mode fields such as TE or TM fields with linear polarization, or circularly polarized (CP) fields with both TE and TM components reduces the maximum gain, and so optimum shapes cannot be found for this case.

II. Maximum Gain for Rotationally Symmetric Broadside Antennas

Consider an arbitrary antenna located about the origin of the coordinate system shown in Fig. 1. If the electric and magnetic vector potentials **F** and **A** are considered to be $\hat{r}$ directed only, then all fields radiating from an arbitrary antenna can be expressed in terms of **F** and **A**. If F_r and A_r are expanded in a Fourier–Legendre series of outward-traveling waves (with time convention $e^{j\omega t}$) as

$$A_r=\sum_m \sum_n a_{mn}krh_n^{(2)}(kr)P_n^m(\cos\ \theta)\ \cos\ (m\phi+\alpha_{mn})$$

$$F_r=\sum_m \sum_n b_{mn}krh_n^{(2)}(kr)P_n^m(\cos\ \theta)\ \cos\ (m\phi+\beta_{mn}), \quad (1)$$

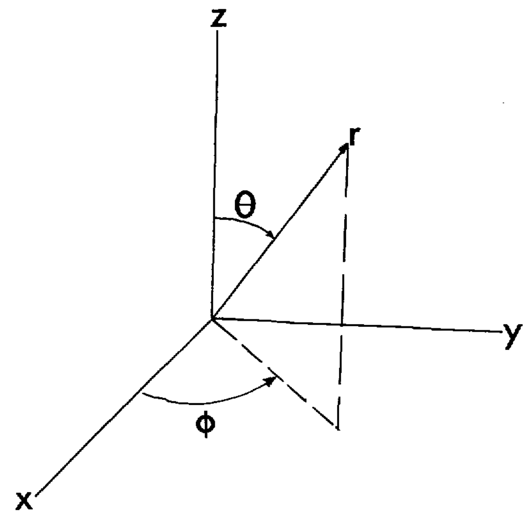

Fig. 1. The spherical coordinate system.

then the coefficients a_{mn}, b_{mn}, α_{mn}, and β_{mn} specify all of the fields outside the antenna with Maxwell's equations. The gain is defined by

$$G \triangleq \frac{4\pi r^2(\mathbf{E}\times\mathbf{H}^*)|_{\text{max pt.}, r\to\infty}}{\iint (\mathbf{E}\times\mathbf{H}^*)|_{r\to\infty} r^2\ \sin\ \theta\ d\theta\ d\phi}. \quad (2)$$

Specializing the above equations to describe a rotationally symmetric broadside antenna requires that the point of maximum power density be at $\theta = \pi/2$, and that the beam maximum does not vary with ϕ. Then the coefficients determining the fields become $a_n = a_{0n} \cos \alpha_{0n}$ and $b_n = b_{0n} \cos \beta_{0n}$ [4].

Maximizing the gain for the the rotationally symmetric ($m = 0$) broadside case ($\theta = \pi/2$ at point of maximum power density) as a function of the coefficients results in [4]

$$\eta a_n = b_n = \frac{P_n^1(0)(2n+1)j^{-n}}{n(n+1)}\ c, \quad (3)$$

where c is a normalization constant and insures that G, a_n, and b_n are real. With the a_n and b_n from (3),

$$G_{\max}(N) = \sum_{n=1}^{N} \frac{(2n+1)}{n(n+1)} (P_n^1(0))^2 = \sum_{\substack{n=1\\ \text{odd}}}^{n} \frac{2n+1}{n(n+1)} \cdot \frac{1}{2^{n-1}} \left(\frac{n!!}{\left(\frac{n-1}{2}\right)!} \right)^2 \quad (4)$$

for an antenna radiating modes only as high as $n = N$ ($n!! = n(n-2)(n-4) \cdots 3\cdot 1$.)

To synthesize antennas having the gain given by (4), using the characteristic mode method, it is necessary to specialize the fields given by (1) to either TE to $\hat{r}$ (TE) or TM to $\hat{r}$ (TM).

For the TE case, (1) becomes

$$A_r = 0$$

$$F_r = \sum_n b_n krh_n^{(2)}(kr)P_n(\cos\ \theta) \quad (5)$$

Manuscript received July 9, 1985; revised September 16, 1985. This work was supported by Grant ECS 8352325 from the National Science Foundation.

The authors are with the Department of Electrical and Computer Engineering, University of Massachusetts, Amherst, MA 01003.

IEEE Log Number 8406407.

0018-926X/86/0200-0254$01.00

where b_n, given by (3), yields the maximum gain in (4). From (5), the fields are

$$E_\theta = E_r = H_\phi = 0$$

$$E_\phi = \sum_{n=1}^{N} b_n h_n^{(2)}(kr) P_n^1(\cos\theta)$$

$$H_r = \frac{1}{jkr\eta} \sum_{n=1}^{N} b_n h_n^{(2)}(kr)(n+1) \left[\frac{P_{n-1}^1(\cos\theta) - \cos\theta P_n^1(\cos\theta)}{\sin\theta} \right]$$

$$H_\theta = \frac{1}{jkr\eta} \sum_{n=1}^{N} b_n [(n+1) h_n^{(2)}(kr) - kr h_{n+1}^{(2)}(kr)] P_n^1(\cos\theta) \quad (6)$$

where the b_n, given by (3), are always real and the choice $c = j\sqrt{30/G_{\max}}$ normalizes the total radiated power to 1 W.

Similarly, for the TM case, (1) becomes

$$F_r = 0$$

$$A_r = \sum_n a_n kr h_n^{(2)}(kr) P_n(\cos\theta) \quad (7)$$

where a_n, given by (3), yields the maximum gain in (4). From (7), the fields are

$$E_\phi = H_\theta = H_r = 0$$

$$H_\phi = -\frac{1}{j\eta} \sum_{n=1}^{N} a_n h_n^{(2)}(kr) P_n^1(\cos\theta)$$

$$E_r = \frac{1}{kr} \sum_{n=1}^{N} a_n n(n+1) h_n^{(2)}(kr) P_n(\cos\theta)$$

$$E_\theta = \frac{1}{kr} \sum_{n=1}^{N} a_n [n h_n^{(2)}(kr) - kr h_{n-1}^{(2)}(kr)] P_n^1(\cos\theta) \quad (8)$$

where the a_n given by (3), are always real and the choice $c = j\sqrt{30/G_{\max}}$ normalizes the total radiated power to 1 W.

III. Optimum Shape Synthesis Using Characteristic Mode Theory

As shown by Garbacz and Pozar [5], [6], outward propagating fields satisfying the conjugate point symmetry condition can be generated by a characteristic surface S with the real currents $J_{\tan}|_S$ out of phase with the fields $\mathbf{E}_{\tan}|_S$ by a constant α. When synthesizing the antennas to radiate the fields given by (6) and (8), α was chosen to be 180°. This yields an antenna for which the Poynting vector is directed outward, normal to the surface at every point on the surface. This condition implies that the radiator is optimum in some sense. For example, if the finite conductivity of the antenna surface is considered, the outward directed Poynting vector of a characteristic field will minimize power loss in the conductor. In addition, the resulting antenna has $Q = 0$ [6] at the one frequency chosen here by setting k to some constant value. For all the following antennas, k is set equal to 1.0.

To synthesize the TE antenna radiating the fields given in (6), an expression for the fields inside the antenna must be found. Taking the standing wave fields inside the antenna to be given by (6) with the spherical Hankel functions $h_n^{(2)}(kr)$ replaced by spherical Bessel functions $j_n(kr)$, as in [5], insures that $J_{\tan}|_S$, given by

$$J_{\tan}|_S = \hat{\mathbf{n}}|_S \times (H^{\text{out}} - H^{\text{in}})|_S, \quad (9)$$

is real and that $\mathbf{E}_{\tan}|_S$ will be continuous.

The surface S is defined by

$$\text{Im}\,\{\mathbf{E}_{\tan}\} = \text{Im}\,\{\hat{\phi} E_\phi\} = 0. \quad (10)$$

For each value of θ, $r(\theta)$ is found from (10) by a root searching procedure. There is a denumerably infinite set of curves $r(\theta)$ for each value of N.

Fig. 2 shows the first few contours generated for the TE, $N = 7$ case. Since the fields are rotationally symmetric, as well as symmetric about $\theta = 90°$, the three-dimensional antenna shape is found by rotating the curves $r(\theta)$ about the z-axis. Observe that the smallest two contours in Fig. 2 do not represent continuous closed shapes, and so are not considered realizable (this effect was also noted in [5]). The surfaces r_1 and r_2 in Fig. 2 are not closed, that is they do not exist for all values of θ. Therefore, the definition of inside fields and outside fields required for the characteristic mode shape synthesis does not make sense (as there is no inside). The remaining curves shown in Fig. 2 $\{r_3, r_4, \cdots\}$ are closed and are valid solutions to (10). Any antenna shape built in between the solutions $\{r_n(\theta)\}$ (i.e., not a solution to (10)) would have a Poynting vector with components directed tangential to or into the surface, and therefore would be less desirable. The smallest continuous contour is selected from the set $\{r_n(\theta)\}$, and is drawn as a solid line in Fig. 2. The smallest closed TE surfaces for $N = 1, 5, 9, 13$, and 15 are shown in Fig. 3. The corresponding surface currents and gains are shown in Figs. 4 and 5, respectively. Observe that the shapes become more and more elongated as N increases, and the current distributions become more uniform. This may suggest that a uniformly fed wire antenna is close to an optimum omnidirectional radiator.

To synthesize the TM antenna radiating the fields given by (8) the standing wave fields inside the antenna are once again found by replacing the spherical Hankel functions by spherical Bessel functions. As above, $J_{\tan}|_S$ will be real and $\mathbf{E}_{\tan}|_S$ will be continuous. Again, the surface S is defined by

$$\text{Im}\,\{\mathbf{E}_{\tan}\} = \text{Im}\,\{(t_r E_r + t_\theta E_\theta)\hat{\mathbf{t}}\} = 0, \quad (11)$$

where $E_{\tan}$ is the dot product of $\mathbf{E}$ with the unit vector $\hat{\mathbf{t}}$ tangent to S and perpendicular to $\hat{\phi}$ at the point (r, θ) on S. As in [5], the tangent vector was approximated by the vector connecting some other, known, nearby point on S to the presently considered (r, θ). Therefore, to determine a point on S requires that the tangent, or at least one point on S, be known already. At $\theta = 0°$ it is assumed that $t_\theta = 1$ and $t_r = 0$ (implying that S does not have a cusp at $\theta = 0°$), then r at $\theta = 0°$ can be found and subsequently $r(\theta)$ by a search procedure. For $N = 1, 5, 9, 13$, and 15 the smallest continuous TM antenna surfaces are shown in Fig. 6, and the corresponding surface currents and gains are shown in Figs. 7 and 5, respectively.

In Fig. 8 gain, which is the same for both the TE and TM cases, is shown as a function of N. As $N \to \infty$, $G(N)$ approaches the gain of a uniform current distribution line source. See line f in Fig. 8. Notice that the maximum gain obtained by the shapes in Figs. 3 and 6 are maximum as a function of N and not maximum as a function of ka. Generally, an antenna of size ka can easily radiate the spherical modes 1 through $N = ka$ and the higher order modes are rapidly cut off. The antennas shown in this communication, however, will theoretically radiate exactly N modes, where $N < ka$. Practically, if these antennas were to be built, the currents in Figs. 4 and 7 could not be excited independently of other modes. In this case, modes of order greater than N would be radiated and would either subtract from or add to the gain.

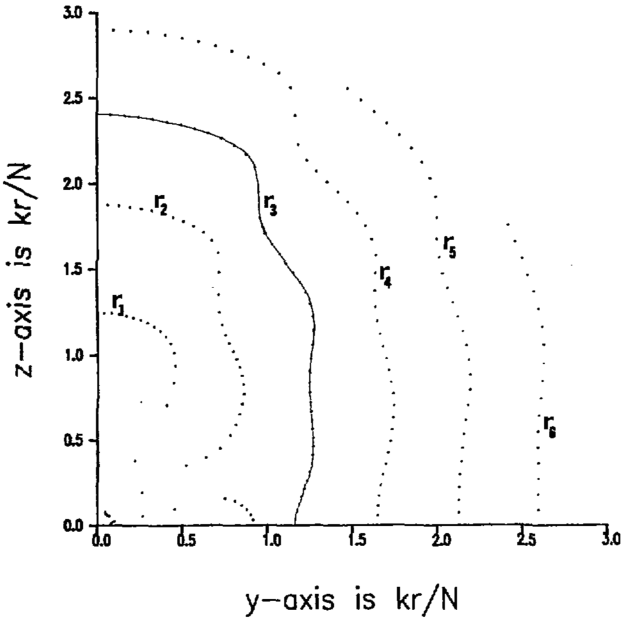

Fig. 2. All $N = 7$ antennas found in a $kr = 3.0$ radius. Solid curve $r_3(\theta)$ is the smallest continuous contour.

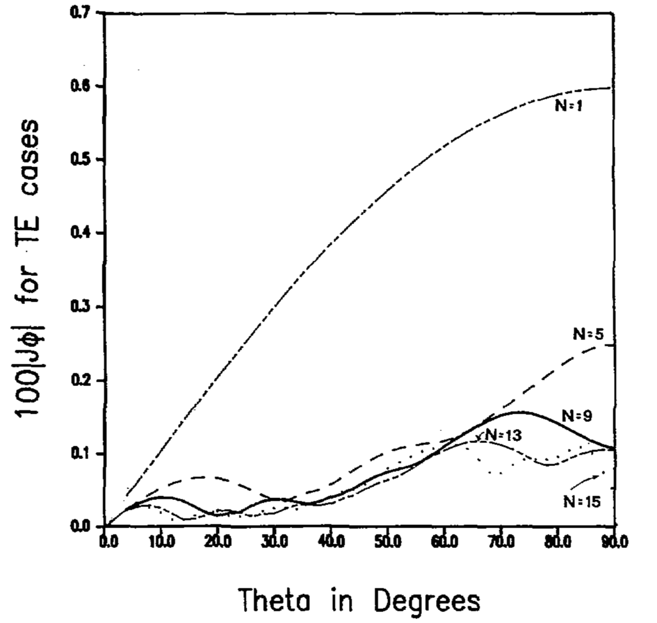

Fig. 4. $J_{\tan}|_S$ versus θ for the TE $N = 1, 5, 9, 13$, and 15 antennas in Fig. 3.

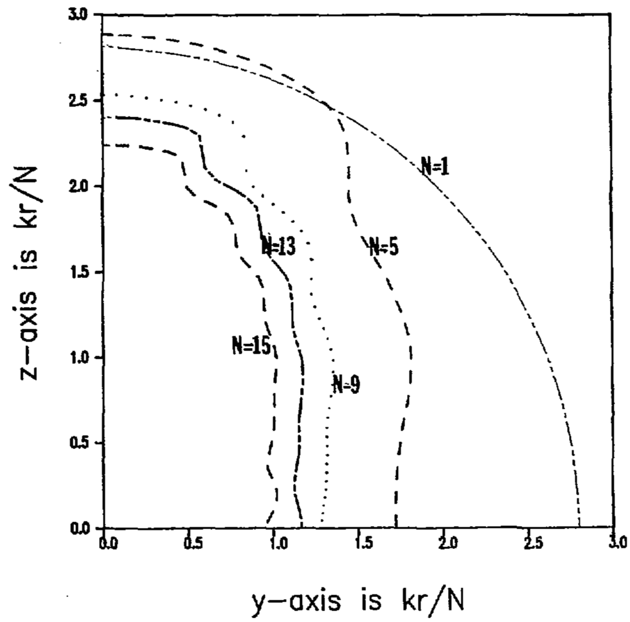

Fig. 3. Smallest continuous antenna surfaces for the TE $N = 1, 5, 9, 13$, and 15 cases.

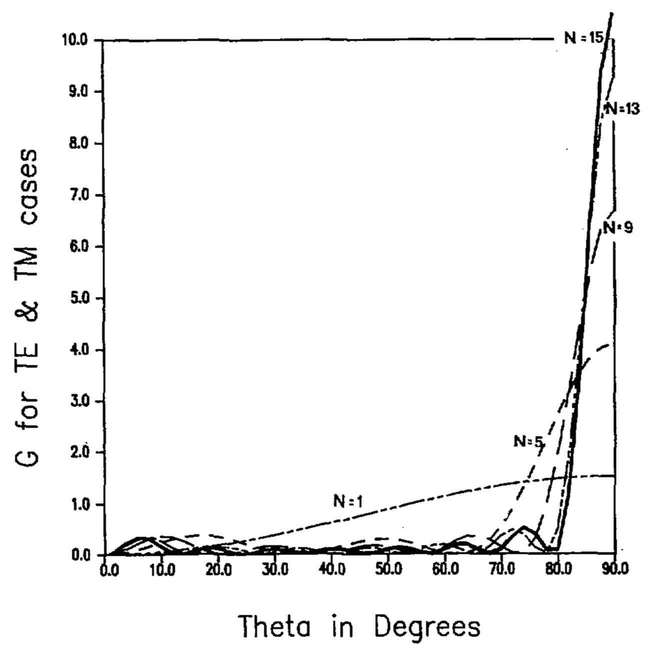

Fig. 5. Gains versus θ for TE or TM $N = 1, 5, 9, 13$, and 15 antennas shown in Figs. 3 and 7. Value at $\theta = 90°$ is same as $G_{\max}$ of (4).

IV. Why No Optimum Shape Exists for the Endfire Case

Consider again an antenna located about the origin in Fig. 1. A general expression for its gain given in (2) can be specialized to the endfire case by letting the point of maximum power density be at $\theta = 0°$, the end of the antenna. Notice the fields are not necessarily rotationally symmetric for the endfire case, and the fields which yield maximum gain consist of both TE and TM fields.

Beginning with (1) and (2) and maximizing the gain for the endfire case (maximum power density at $\theta = 0°$) [1], [2] leads to $a_{mn} = b_{mn} = \alpha_{mn} = \beta_{mn} = 0$ for $m \neq 1$. For the $m = 1$ coefficients the equations analogous to (3) are

$$\eta a_{1n} = b_{1n} = j^{-n}(2n+1)c/(3n(n+1))$$

and

$$\alpha_{1n} = \beta_{1n} + \pi/2, \tag{12}$$

which specify linear polarization. The gain is

$$G_{\max} = N^2 + 2N. \tag{13}$$

See curve a in Fig. 8 for a plot of this $G_{\max}$.

Using the coefficients of (12) yields **H**-fields outside of the antenna which when subtracted from their standing wave counterparts inside the antenna do not in general yield a real surface current, as in the previous case. This may be expected, however, since the conjugate point symmetry property is not satisfied by the far-field pattern [5]. In an attempt to meet this conjugate point symmetry requirement, TE,

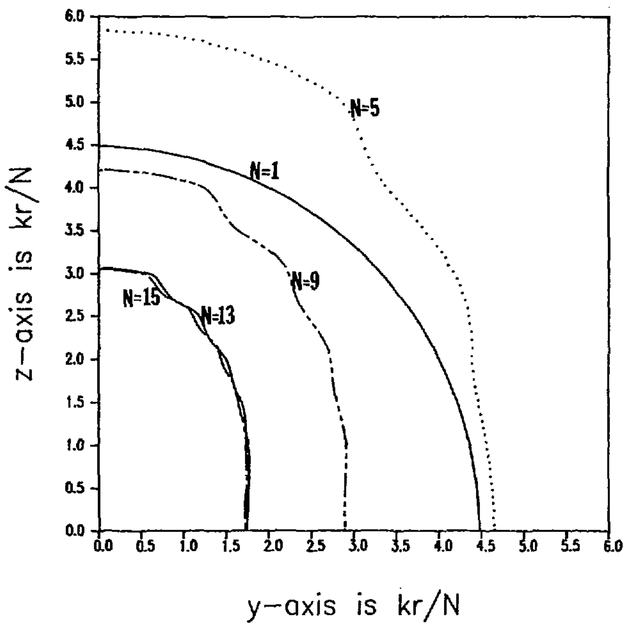

Fig. 6. Smallest continuous antenna surfaces for the TM $N = 1, 5, 9, 13$, and 15 cases.

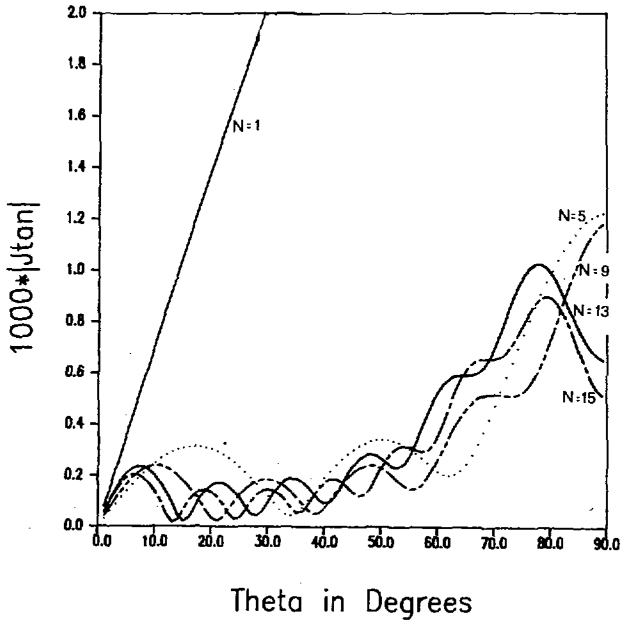

Fig. 7. $J_{\tan}|_S$ versus θ for the TM $N = 1, 5, 9, 13$, and 15 antennas in Fig. 6.

TM, and circularly polarized (CP) fields were considered individually.

For the TE case with linear polarization, (12) becomes

$$\eta a_{1n} = 0$$

$$b_{1n} = j^{-n}(2n+1)c/(3n(n+1))$$

and

$$\beta_{1n} = 0. \tag{14}$$

For the TM case with linear polarization, (12) becomes

$$b_{1n} = 0$$

$$\eta a_{1n} = j^{-n}(2n+1)c/(3n(n+1))$$

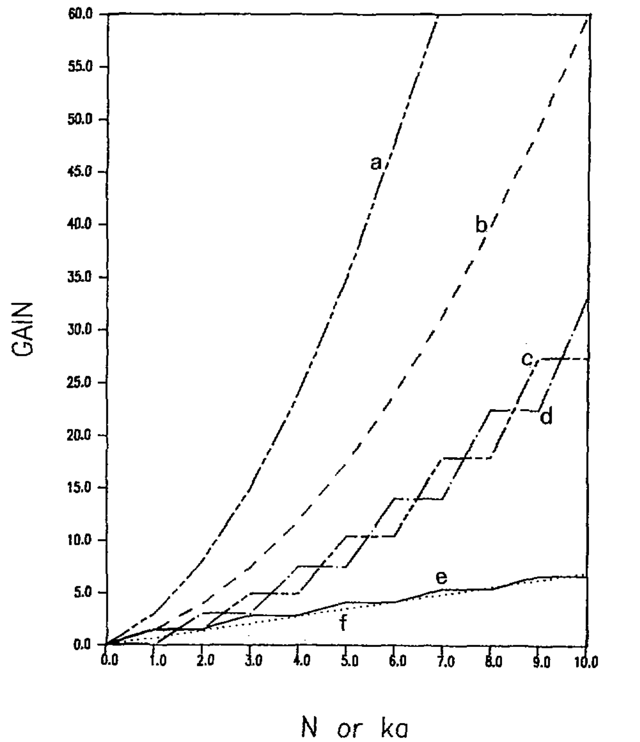

Fig. 8. Comparison of endfire gains with maximum omnidirectional gain. a: $G_{\max}$ versus N, endfire. b: $G_{\max}/2$ versus N, double-endfire. c: Odd double-endfire gain versus N. d: Even double-endfire gain versus N. e: $G_{\max}$ versus N, rotationally symmetric broadside. f: Approximate G for a uniform line source versus ka (dashed line).

and

$$\alpha_{1n} = \pi/2. \tag{15}$$

For the CP case with both TE and TM components, (12) becomes

$$\eta a_{1n} = \pm j b_{1n} = j^{-n}(2n+1)c/(3n(n+1))$$

and

$$\alpha_{1n} = \beta_{1n} = 0, \tag{16}$$

where the plus sign or minus sign signifies left-hand circularly polarized (LHCP) or right-hand circularly polarized (RHCP) circular polarization. Specializing the equations as above to describe only TM, TE, RHCP, or LHCP endfire cases leads in all cases to maximum radiation off both ends ($\theta = 0°$ and $\theta = 180°$, double-endfire) and to a gain that is 1/2 the $G_{\max}$ of (13). See curve b in Fig. 8 for a plot of this gain. In these cases $J_{\tan}$ cannot be made real everywhere except for the $N = 1$ antenna, which is a sphere.

Breaking the above double-endfire cases into even (i.e., nonzero coefficients given by (14), (15), or (16) for only even values of n) and odd (i.e., nonzero coefficients given by (14), (15), or (16) for only odd values of n) mode antennas reduces the gain still further, but at least yields antennas that can finally be synthesized with a single characteristic surface. Therefore, to generate the maximum gain endfire fields requires four characteristic antennas: either 1) odd mode TE, 2) even mode TE, 3) odd mode TM, and 4) even mode TM; or 1) odd mode RHCP, 2) even mode RHCP, 3) odd mode LHCP, and 4) even mode LHCP. Each of these cases has its own characteristic shape, so it does not make sense to think of a superposition of these results. The gains for these odd and even mode antennas are plotted as curves c and d in Fig. 8.

V. Conclusion

Although the antennas synthesized in Section III were only for N as high as 15, the same method can produce antennas for any N. The trend in the antenna surfaces and currents is to have more and smaller perturbations from a smooth contour as N gets larger. Each rotationally symmetric broadside antenna in Section III has maximum gain for the number of modes it radiates and is optimum in the sense that power loss is minimized in the conductor surface of the antennas. It is also optimum in that $Q = 0$ at the frequency $k = 1.0$. This is more restrictive than just the low Q condition $ka = N$ and may explain why here ka is greater than N.

It is impossible to find a single endfire antenna shape that has maximum gain for the number of modes it radiates and is optimum in that the Poynting vector is directed outward, normal to the surface at every point on the surface, because such an antenna requires the nonrealizable superposition of four different surfaces. As shown in Section IV, one characteristic endfire antenna produces only about 1/4 the maximum endfire gain.

As a practical matter it would be difficult to build such optimum shape antennas, primarily because of the problem in exciting only one characteristic mode. A conductor in the shape of Figs. 3 or 6, for example, possesses an infinite set of characteristic modes, only one of which gives rise to the desired maximum gain fields. The problem is then to excite this mode, while minimizing the excitation of other modes.

References

[1] R. F. Harrington, "Effect of antenna size on gain, bandwidth, and efficiency," *J. NBS-D*, vol. 64D, no. 1, pp. 1-12, Jan.-Feb. 1960.

[2] ——, *Time-Harmonic Electromagnetic Fields*. New York: McGraw-Hill, 1966.

[3] ——, "On the gain and beamwidth of directional antennas," *IRE Trans. Antennas Propagat.*, vol. AP-6, pp. 219-224, July 1958.

[4] L. J. Chu, "Physical limitations of omni-directional antennas," *J. Appl. Phys.*, vol . 19, pp. 1163-1175, Dec. 1948.

[5] R. J. Garbacz and D. M. Pozar, "Antenna shape synthesis using characteristic modes," *IEEE Trans. Antennas Propagat.*, vol. AP-30, no. 3, pp. 340-350, May 1982.

[6] R. J. Garbacz, "A generalized expansion for radiating and scattered fields," Ph.D. dissertation, Ohio State Univ., 1968.

An Anisotropic Turbulence Model for Wave Propagation Near the Surface of the Earth

ROBERT M. MANNING, MEMBER, IEEE

Abstract—**A model of turbulent anisotropy of refractive index fluctuations near the surface of the earth is presented and used to calculate the mutual coherence function (MCF) of a propagating plane wave. It is found that there are measurable differences in the transverse (horizontal and vertical) MCF's thus making possible active remote sensing of turbulent anisotropy.**

Manuscript received July 16, 1985; revised September 5, 1985. This work was supported by the U.S. Army Research Office under Contract DAA6 29081-R-0172. This work was presented at the 1985 North American Radio Science Meeting and International IEEE/Antennas and Propagation Society Symposium, Vancouver, British Columbia, Canada, June 17-21, 1985.

The author is with the Department of Electrical Engineering and Applied Physics, Case Western Reserve University, Cleveland, OH 44106.

IEEE Log Number 8406404.

I. Introduction

In the theoretical description of wave propagation in a turbulent (random) atmosphere, one usually assumes that the associated refractive index fluctuations are isotropic. This is probably a good approximation if one is interested in propagation through those portions of the atmosphere that are sufficiently removed from the earth's surface. However, for propagation near the surface of the earth ($\sim$2–4 m above the ground) one can expect deviations of the large scale (small spatial frequency) portions of the turbulence field from the ideal isotropic situation due to the interaction of the moving atmosphere with the fixed boundry of the ground. (However, for the small scales (large spatial frequencies) of the turbulence field, i.e., scale lengths that are much smaller than their height above the ground, isotropy will exist on this "local" level [1].) In particular, turbulent outer scale lengths should tend to be elongated in the horizontal direction along the earth as has been recently observed [2].

It is the purpose of this work to present a simplified and calculationally expedient model of the anisotropic nature of the refractive index field alluded to in the above discussion. This model will then be used to show that there will exist measureable differences in the horizontal and vertical one-dimensional mutual coherence functions (MCF's) of a plane wave propagating near the earth's surface. Thus, comparison of perpendicular MCF measurements in an experimental situation [3] can lead to the verification of anisotropy of the turbulence field of the atmosphere and, within the context of this model, allows the active remote determination of the particular parameters characterizing anisotropy.

II. Anisotropic Turbulence Model

The model chosen to describe the anistropy of the turbulence field near the earth's surface employs the usual isotropic Kolmogorov spectrum with an elliptical anisotropic background, the semimajor axis of which is parallel to the ground. Such a form of anisotropy was considered in [4]. The anisotropic background is taken to decay exponentially with increasing spatial frequency. Thus, letting ϕ be an orientation angle measured from the axis parallel to the earth, from which general angular displacements θ are reckoned, and letting the parameters a and α be constants that characterize the anisotropy, one has for an anisotropic turbulence spectrum

$$\Phi(\kappa,\ \theta;\ \phi)=\Phi_I(\kappa)[1+a\ \exp\ (-\alpha^2\kappa^2)\ \cos\ (2\theta+2\phi)] \tag{1}$$

where

$$\Phi_I(\kappa)=0.033\,C_n^2\kappa^{-11/3} \tag{2}$$

is the spectrum of isotropic turbulence, κ is the spatial frequency of the refractive index fluctuation sizes, and C_n^2 is the structure parameter of these fluctuations. (This not the most general form that can be considered; the coefficient a could also be taken as a function of κ and/or θ. However, due to a lack of experimental information on this aspect of the problem, the quantity a will be taken as a constant here.)

The constants a and α can be determined from currently known data [2]. At a height H above the earth, the outer scale of turbulence L_{OH} horizontal to the earth's surface is given by

$$L_{\mathrm{OH}}=0.8H \tag{3}$$

and that vertical to the earth L_{OV} is

$$L_{\mathrm{OV}}=0.4H. \tag{4}$$

It must be remembered that although not stated explicitly in [2], (3)

0018-926X/86/0200-0258$01.00